Defence Science Journal, Vol. 73, No. 4, July 2023, pp. 385-393, DOI : 10.14429/dsj.73.17481

Effect of Localised Pressure Depression and Rain on Aerodynamic Characteristics of MALE UAV

M. Vijayakumar[#,*], K.M. Parammasivam[$], S. Rajagopal[#] and C. Balaji[!]

[#]*DRDO-Aeronautical Development Establishment, Bengaluru - 560 075, India*
[$]*Department of Aerospace Engineering, Anna University, Chennai - 600 025, India*
[!]*Senior Scientist, Metacomp Technologies Pvt. Ltd., Chennai - 600 020, India*
[*]*E-mail: mvijaykumar.ade@gov.in*

ABSTRACT

This paper presents the effect of the local low-pressure region in the atmosphere and rain on aerodynamic characteristics of medium altitude long endurance unmanned aerial vehicle (MALE-UAV) configuration during cruise/loiter. Computations are performed using CFD++, a commercial CFD software suite. A large low-pressure depression past the MALE UAV (symmetrically and asymmetrically) with pressure 10 – 15 % lower than the free stream pressure and a widespread rainfall type with a rainfall rate of 1195 mm/hr., are considered for CFD simulation. A large low pressure that spans the whole MALE-UAV results in a decrement in both lift and drag, but does not affect the yawing and rolling moments significantly. However, a low-pressure region that engulfs only one-half of MALE UAV causes sudden/abrupt changes in rolling and yawing moments. The effect of rain causes a significant decrease in a lift at higher alpha, accompanied by a decrease in stall angle of 2 degrees, and a significant increase in drag. From the study, a Standard Operating Procedure (SOP) was adopted to fly UAVs in adverse weather effects, such that the aircraft can be operated with a velocity higher than 1.3Vstall and at a power setting not less than 75% of max power capacity.

Keywords: MALE (Medium Altitude Long Endurance)-UAV(Unmanned Aerial Vehicle); Low-pressure depression; Rain; Eulerian dispersed phase model(EDP); Adverse weather effects

NOMENCLATURE

C_L : Coefficient of lift
C_D : Coefficient of drag
C_m : Coefficient of pitching moment
C_y : Side force coefficient
C_l : Rolling moment coefficient
C_n : Yawing moment coefficient
P : Static pressure
α : Angle of attack
β : The angle of side slip
C_P : Coefficient of pressure

1. INTRODUCTION

An UAV is required to operate in various weather conditions. A typical MALE-UAV has to operate for more than 20 hrs during its mission and may have to cover more than 500 km distance. This may require it to fly in various unexpected adverse conditions. Typical adverse conditions expected during the flight are rain, icing, turbulence, low-pressure packet, gust, etc.,[1]. Various studies have been carried out for manned aircraft and safe operating standards have been established. Apart from imparting downward and backward momentum, the rainfall reduces visibility, decreases the accuracy of measurement instruments/sensors, erodes aircraft surfaces, and increases fuel consumption [1].

Received : 07 September 2021, Revised : 08 November 2022
Accepted : 03 February 2023, Online published : 11 July 2023

The CFD can play a major role in providing important input for UAV design so that the aerodynamic characteristics of UAV can be predicted and the required preventive or protective steps can be built into its autonomous features. To provide these features, it is required to understand the aerodynamic effect of the adverse phenomena is required. In this paper, the effect of the low-pressure region in the atmosphere and rain on the aerodynamic characteristics of ADE MALE UAV configuration are studied.

2. FLOW CONDITIONS USED FOR CFD SIMULATION

For all the cases reported in this paper, the simulations are carried out for M = 0.125 and altitude 3.69 km for Indian atmospheric conditions (P_{ref} = 64.6 kPa, T_{ref} = 279 K).

2.1 Low-Pressure Depression Simulation

Low-pressure depression studies are performed for an angle of attack (α) 5.6° and without any side slip (β= 0.0°).

2.2 Rain Simulation

For rain simulations, α sweep between -8° to 12° with β= 0.0° is considered.

Rain is typically characterised by its type[1]. A widespread rainfall type with a rainfall rate of 1195 mm/hr (R) is considered. As summarised in Cao[1], *et al.*, given the R, the liquid water content (LWC) in the rain environment can be taken following

Table 1. Rain properties considered for rain simulation[1] at α= 5.6° (Y – Velocity is 0 as side slip angle (β) is 0°)

Rain droplet size (mm)	Fluidised density (kg/m^3)	Number of of droplets/m^3	X – Vel (m/s)	Z – Vel (m/s)
1	0.0015	2896	42.084	0.23
2	0.0050	1198	42.34	-2.43
3	0.0062	495	42.49	-3.92
4	0.0061	205	42.57	-4.71
5	0.0045	85	42.60	-5.10
6	0.0031	35	42.62	-5.28

Figure 1. Surface mesh over MALE UAV.

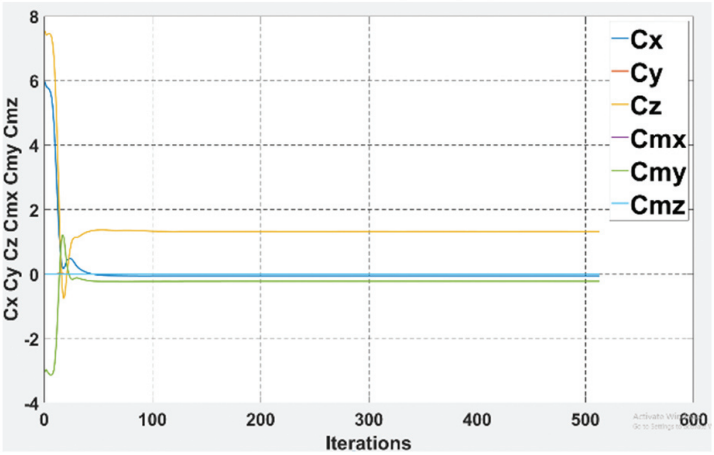

Figure 2. Convergence of forces and moments coefficients with iterations for Steady simulation without low-pressure depression past MALE UAV at α = 5.6°, V = 41.9038 m/s, and Alt = 3.69 km.

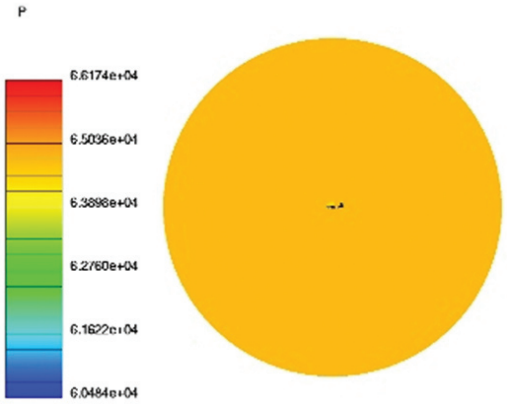

Figure 3. Sectional pressure contour at Y = 0 m (symmetry plane) for MALE UAV without low-pressure box.

Marshall and Palmer[2]. For the current study, LWC is calculated and taken as 30 g/mm^3. The droplet size distribution and the terminal velocity of the droplets are calculated following Joss and Waldvogel[3] and Markowitz[4]. Table 1 summarises the droplet size considered, its partial fluidized density, number density, and its velocity components with due consideration of its terminal velocity in ambient air.

3. GRID AND COMPUTATIONAL DETAILS

The surface mesh over MALE UAV geometry is shown in Fig. 1. The hybrid mesh (combination of Tetrahedron and Penta cells) is generated using Ansys ICEM CFD software. The minimum element size on the aircraft surface is 2 mm and the maximum element size at the far-field is 10 m. The spherical computation domain with a radius of 100 times the mean aerodynamic chord of the wing is considered for simulation. The element size on the aircraft surfaces is between 2 mm to 60 mm depending on location. There are 24 prism layers generated between the surface and Tetrahedron to capture wall shear stress, separation, and stall behavior accurately and also

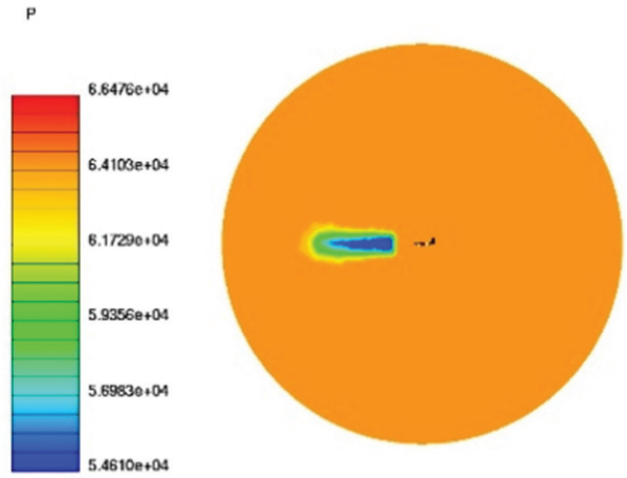

Figure 4. Sectional pressure contour at Y = 0 m (symmetry plane) for MALE UAV with full low-pressure box located 10 m from the fuselage nose.

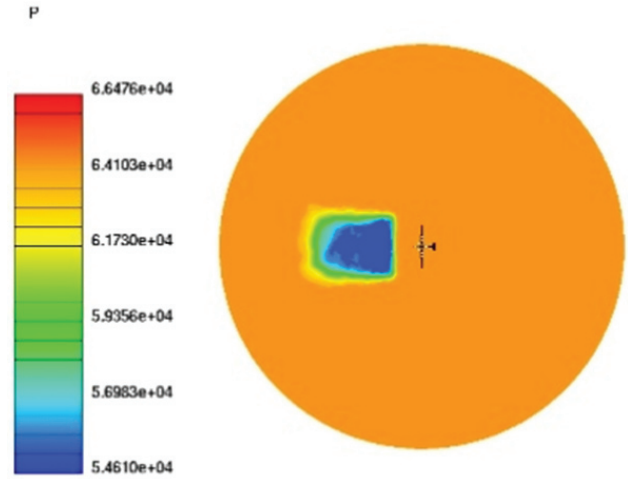

Figure 5. Sectional pressure contour at Z = 0.3 m for MALE UAV with full low- pressure box located 10 m from the fuselage nose. (FRL is at Y = Z = 0 m).

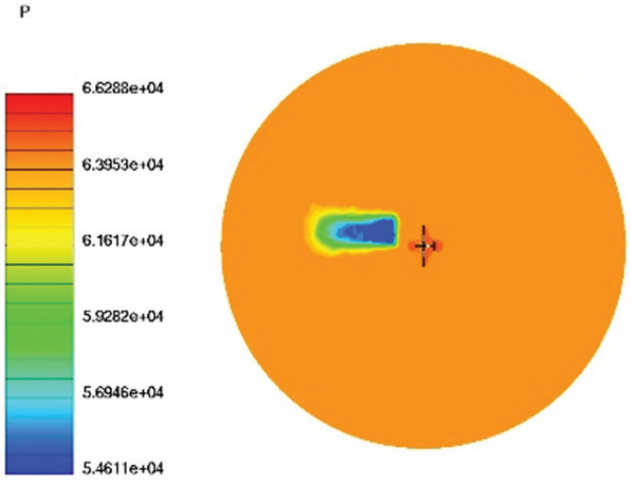

Figure 6. Sectional pressure contour at Z = 0.3 m for MALE UAV with half low-pressure box (FRL to SB side wing) located 10 m from the fuselage nose.

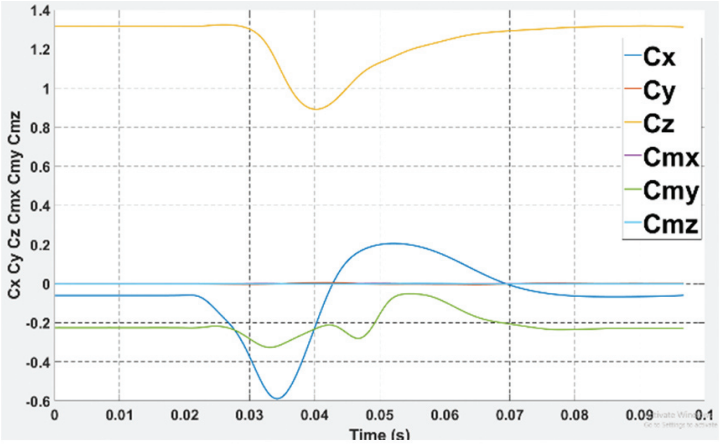

Figure 7. Convergence of forces and moments coefficient with time for the transient simulation with low-pressure depression at α= 5.6°, V = 41.9038 m/sec, and Alt = 3.69 km. (Full - Box introduced at 10.6 m in front of fuselage nose).

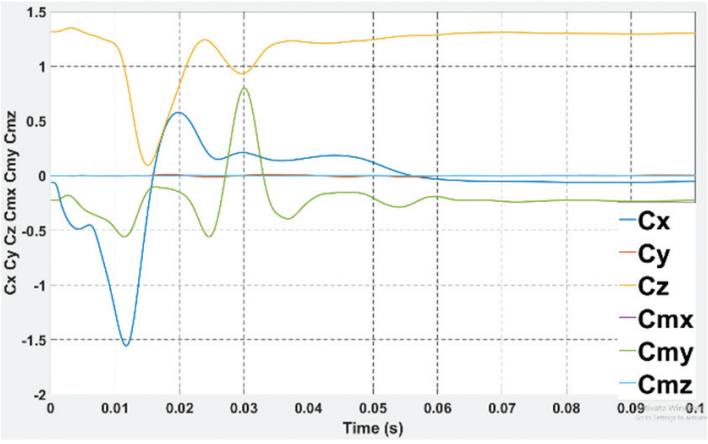

Figure 8. Convergence of forces and moments coefficients with time for the transient simulation with low-pressure depression at α = 5.6°, V = 41.9038 m/sec, and altitude = 3.69 km. (Full - Box introduced in front of the fuselage nose).

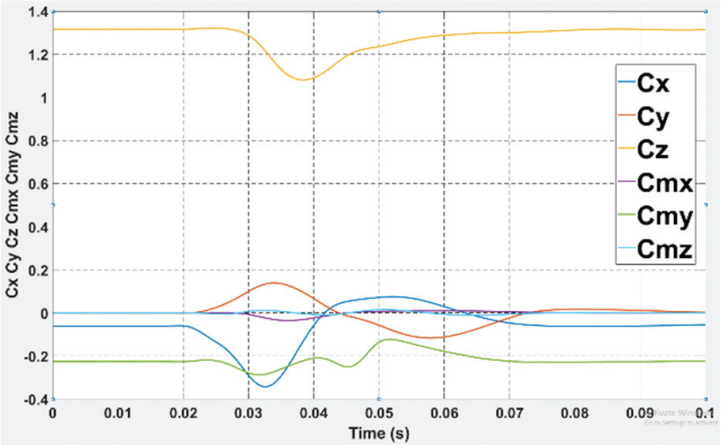

Figure 9. Convergence of forces and moments coefficients with time for the transient simulation with low-pressure depression at α = 5.6°, V = 41.9038 m/sec, and Alt = 3.69 km. (Half - FRL to SB side- Box introduced at 10.6m in front of fuselage nose).

capture boundary layer thickness accurately. The flow domain is discretized with 33 million tetrahedral cells & 31 million Penta cells for MALE UAV configuration. The mesh used for the CFD simulation is arrived through grid independence study carried out by varying surface elements size (coarse = 3/2 times medium mesh surface element size, fine = 2/3 times medium mesh surface element size) and number of prism layers (coarse 18, medium 24 & fine 30 layers).

Computations are performed using CFD++ software suite[5] with preconditioned compressible Navier-Stokes solver and Spalart Allmaras (SA) model used for turbulence closure.

For the low-pressure depression past the MALE UAV, steady simulations are first performed without any imposed pressure depression region. Figures 2 and 3 show the load convergence and the pressure contour field in the symmetry plane for this case. Following this, a low-pressure zone (50 m in length, 6 m in height, and 15 m in one spanwise direction) with pressure 10 – 15 % lower than the free stream pressure is introduced ahead of the MALE UAV configuration, (see Figs. 4-6). Four scenarios are considered,

- The low-pressure region crosses the aircraft symmetrically starting at X = 10.6 m, ahead of the fuselage,
- The low-pressure region crosses the aircraft symmetrically starting at the nose of the fuselage,
- The low-pressure region crosses the aircraft asymmetrically, i.e. one side of the wing, starting at X =10.6 m ahead of the fuselage,
- The low-pressure region crosses the aircraft asymmetrically, i.e. one side of the wing, starting at the nose of the fuselage.

A transient simulation with a time step size of 0.1 ms is then performed for 0.1 s and low-pressure depression is allowed to convect past the MALE UAV. For each time step, twenty internal iterations are considered in order to ensure temporal convergence.

For rain simulation, the presence of water droplets is accounted using Eulerian Dispersed Phase (EDP) formulation[5], allowing for two-way mass, momentum, and energy interactions across the rain droplets and atmospheric air.

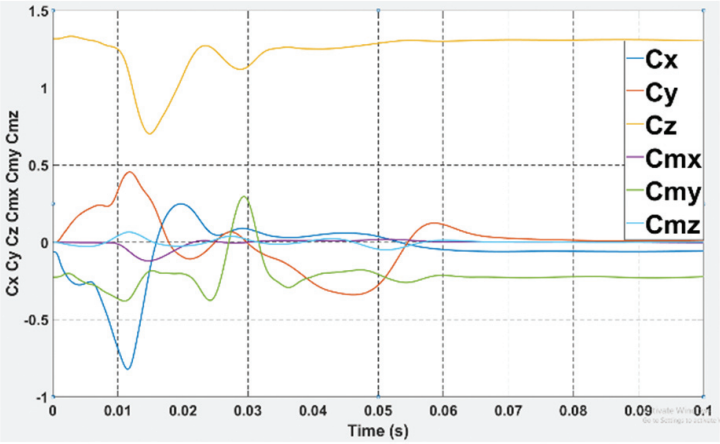

Figure 10. Convergence of forces and moments coefficients with time for the transient simulation with low-pressure depression at $\alpha = 5.6°$, $V = 41.9038$ m/sec, and Altitude = 3.69 km. (Half - FRL to SB side- Box introduced in front of fuselage nose).

Table 2. Incremental aerodynamic force and moment coefficient encountered due to possible low-pressure zone for four scenarios

Parameters	Case-1	Case-2	Case-3	Case-4
ΔC_L	-0.1663	-0.1339	-0.1528	-0.0707
ΔC_D	-0.543	0.1967	-0.2582	0.106
ΔC_m	-0.0887	-0.0962	-0.0384	-0.0352
ΔC_y	0.0004	0.0092	0.1382	-0.1186
ΔC_l	0.0002	-0.0007	-0.0333	0.0117
ΔC_n	0.0001	-0.0017	0.0083	-0.0115

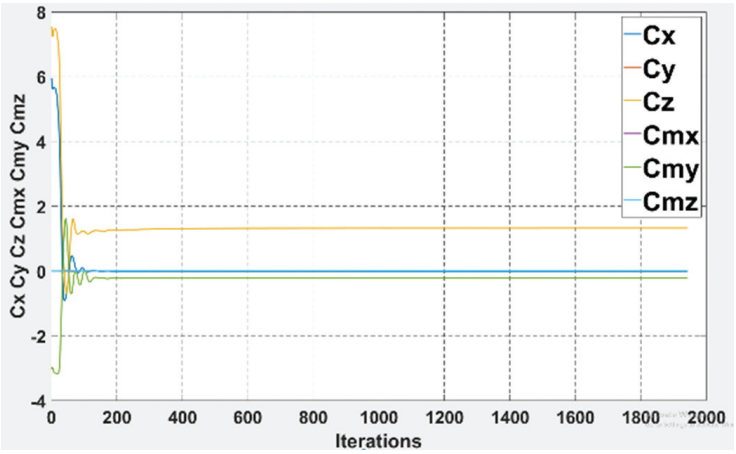

Figure 11. Convergence of forces and moments coefficients with iterations for steady simulation with rain effect for MALE UAV at $\alpha = 5.6°$, $V = 41.9$m/sec, and Alt = 3.69 km.

3.1 Procedure Followed to Estimate Rain Properties Required for Rain CFD Simulation Using Reference[1-4]

- Select the type of rainfall rate using the condition.

$$\text{Rainfall rate } (R) \le 1000 \frac{mm}{hr} - \text{light rain}$$

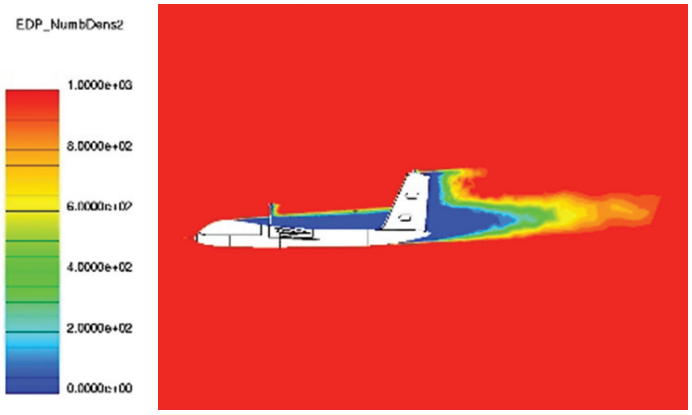

Figure 12. Sectional contour plot showing number density distribution at Y= 0 m for EDP corresponding to 2 mm droplet.

$$\text{Rainfall rate } (R) \ge 1000 \frac{mm}{hr} - \text{heavy rain}$$

- Select the values of N_o & I for different rainfall using the following table.

Type of rainfall	$N_o\ m^{-3}\ mm^{-1}$	$I\ mm^{-1}$
Drizzle (light rain)	30000	$5.7 \times R^{-0.21}$
widespread	7000	$4.1 \times R^{-0.21}$
Thunderstorm	1400	$3.0 \times R^{-0.21}$
Marshall and palmer	8000	$4.1 \times R^{-0.21}$

where,

N_o – Number of droplets per unit volume (Varies with type of rainfall)

I – Size interval (Varies with type of rainfall)

- Select the raindrop diameter (D_p) from 1mm to 6 mm.
- Estimate the number density for each droplet diameter using below the formulae.

$$N(D_p) = N_o \exp(-ID_p)\ (0 \le D_p \le D_{pmax})$$

where,

D_p – Droplet diameter

D_{pmax} – Maximum droplet diameter

$N(D_p)$ – Number of raindrops per unit volume per unit size interval having equivolume spherical diameter D_p (mm).

- Estimate liquid water content LWC for the particular rainfall rate using the below relation

Drizzle = LWC = $0.08928 \times R^{0.84}\ g/m^3$

Widespread = LWC = $0.07782 \times R^{0.84}\ g/m^3$

Thunderstorm = LWC = $0.05430 \times R^{0.84}\ g/m^3$

Marshall & Pamer = LWC = $0.08894 \times R^{0.84}\ g/m^3$,

where, R – Rainfall rate

- Estimate the fluidised density of each droplet for the particular rainfall rate using the following formula

Fluidized density:

$$= N(D_p) \times 1000 \times ((4 \times \Pi) \times (D_p \times 0.5 \times 0.001)^3 \div 3)$$

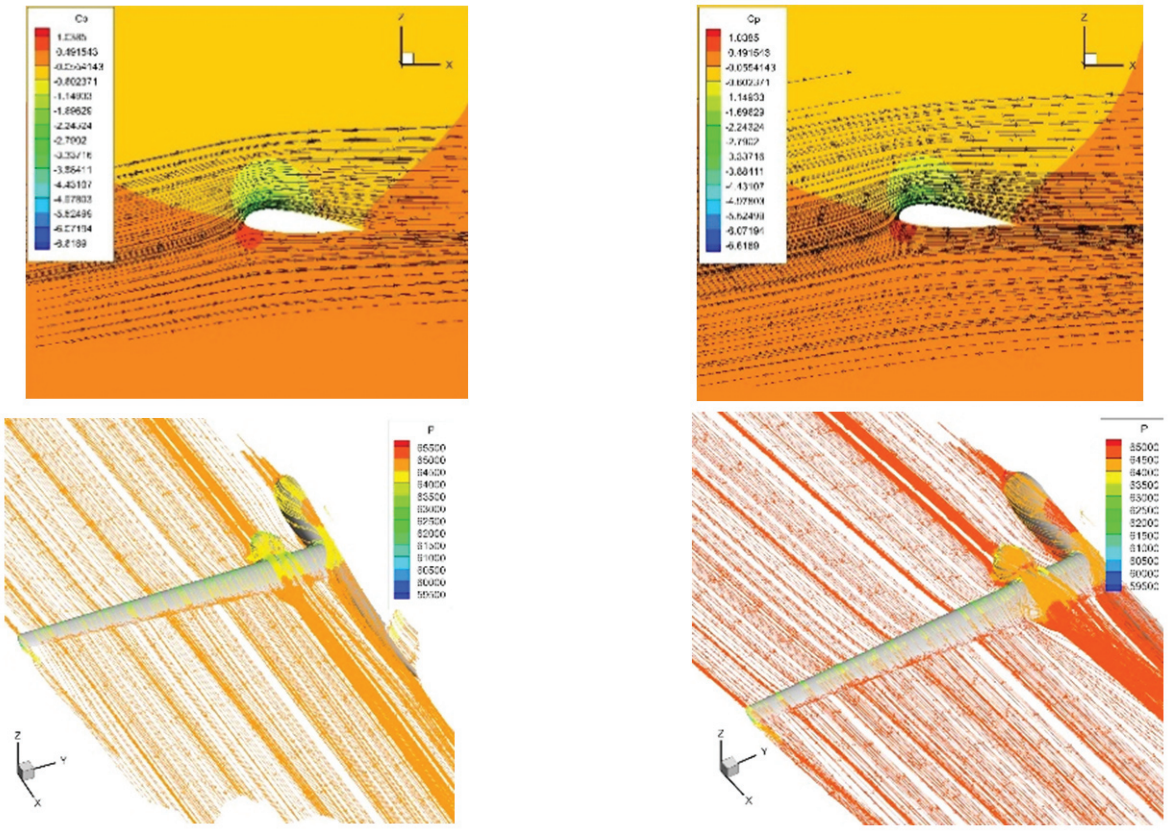

(a) Without rain effect. **(b) With rain effect**

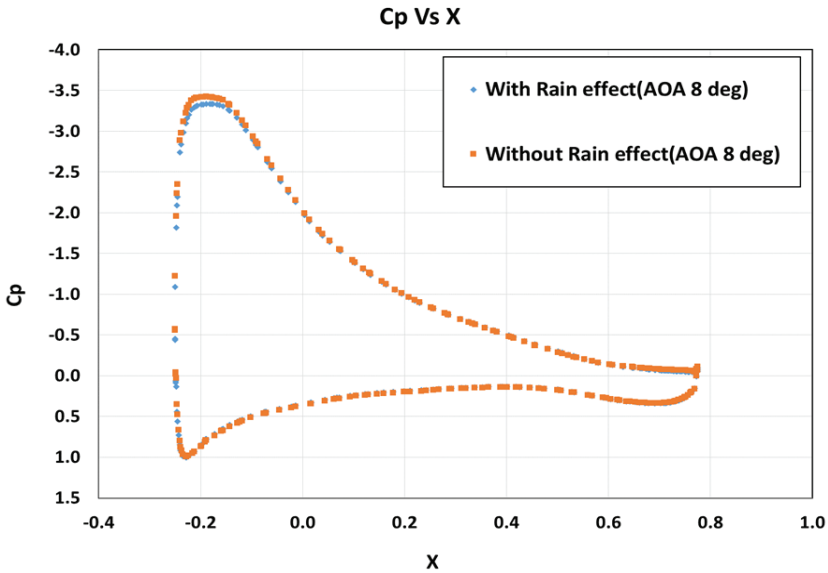

Figure 13. Sectional C_p plot & stream lines pattern at mid-span & top surface of the wing at α = 8°.

- Estimate the terminal velocity of the raindrop

$$V_T(D_p) = 9.58 \times (1 - \exp[-(D_p \div 1.77)^{1.147}])$$

- Estimate horizontal (axial) and vertical components of rainfall Terminal Velocity for each droplet using the below relation.

Horizontal or X - component of $V_T(D_p) =$

$V_T(D_p) \times \sin(a_{aircraft})$

Vertical or Z - component of $V_T(D_p) =$

$-V_T(D_p) \times \cos(a_{aircraft})$

- Estimate the total (combination of air & rain component) horizontal and vertical component of velocity for each droplet for the particular rainfall rate using the below relation.

Total X - component of velocity =

Horizont. or X-comp. of $V_T(D_p) + V_{air} \cos(a_{aircraft})$

Total Z - component of velocity =

Vertical or Z - comp. of $V_T(D_p) + V_{air} \sin(a_{aircraft})$

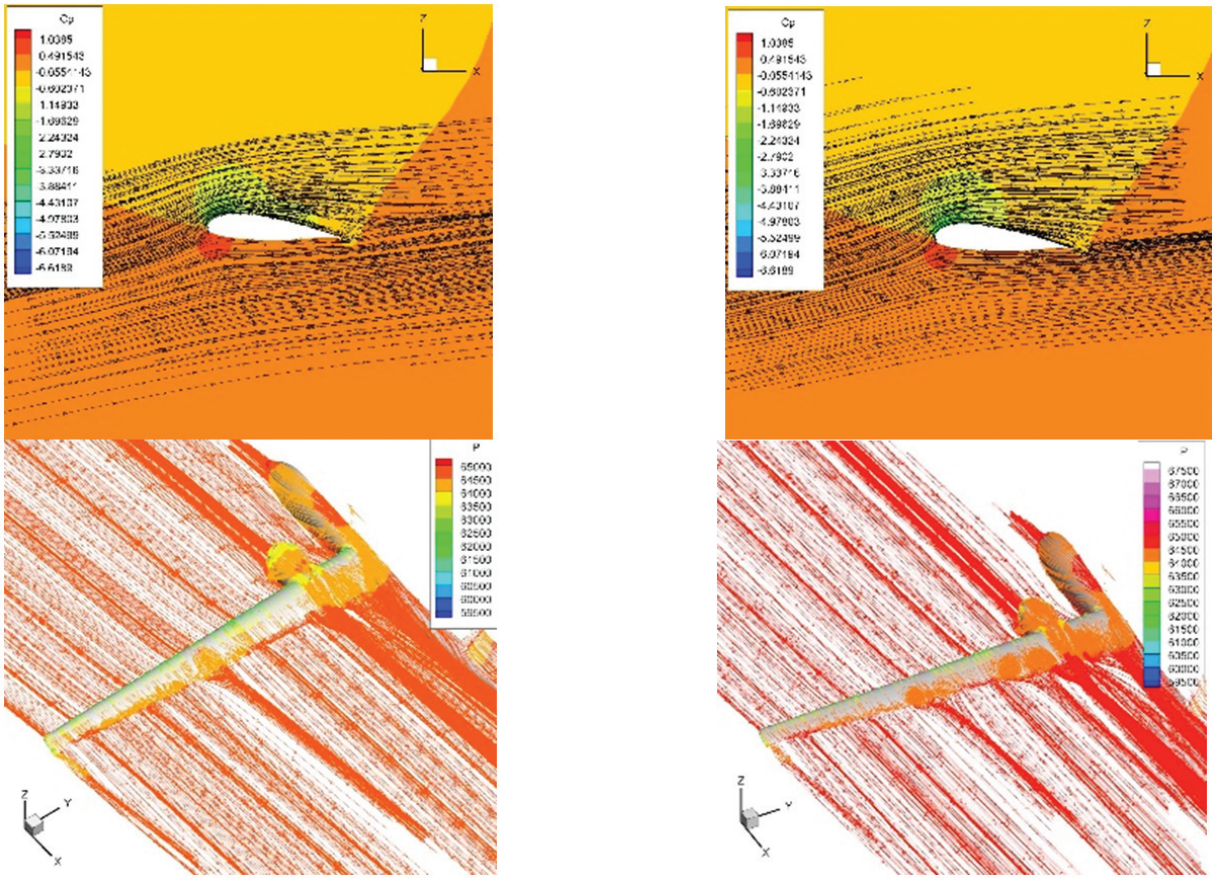

(a) Without rain effect.

(b) With rain effect

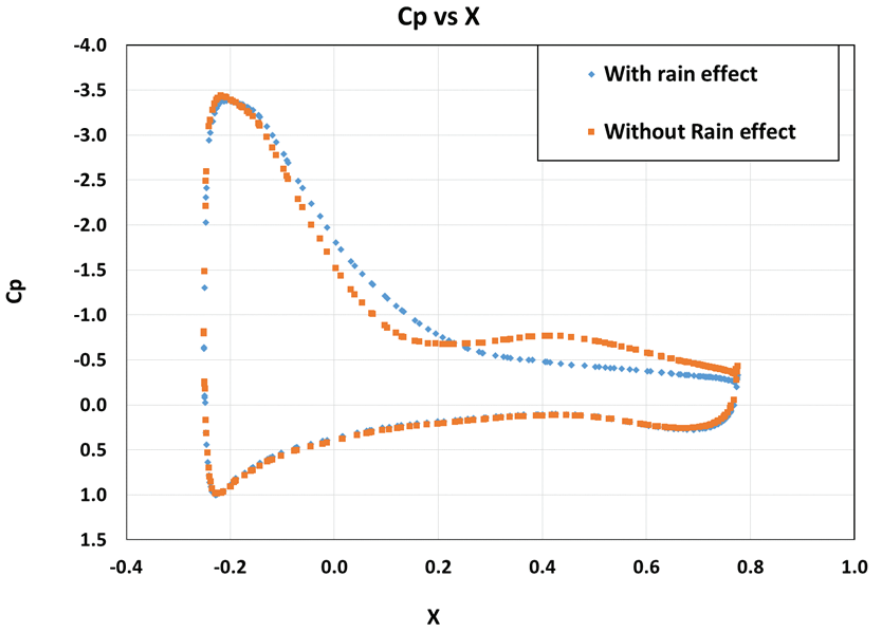

Figure 14. Sectional C_p plot & streamlines pattern at mid-span & top surface of the wing at α = 10°.

4. RESULTS AND DISCUSSION

It is observed that adverse weather simulation has the following effect on the aerodynamic characteristics of MALE UAVs.

4.1 Local Low-Pressure Zone

The local low-pressure zone can change the aerodynamic characteristic momentarily. Figures 7-10 show the variation of forces and moments coefficients when the different type of low-pressure region convects past the MALE-UAV. The Incremental aerodynamic force and moment coefficient for the four cases are given in Table 2.

Based on the CFD analysis carried out, it is observed that there is a sudden drop in lift and drag when the localized pressure

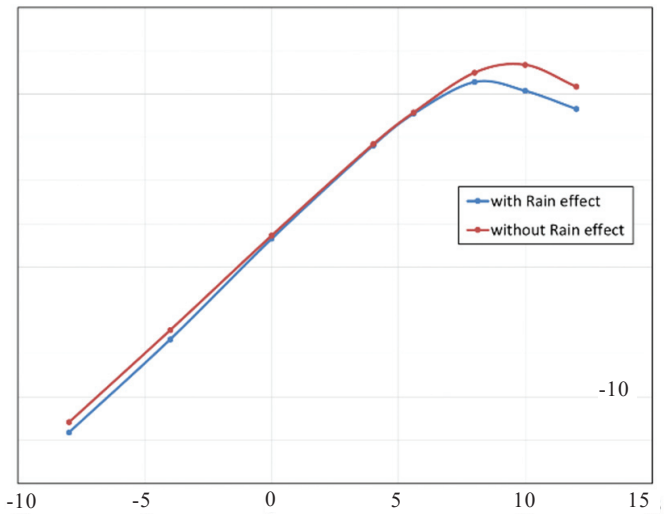

Figure 15. C_L vs. α with & without rain effect for MALE UAV at V = 41.9 m/s, Alt = 3.69 km.

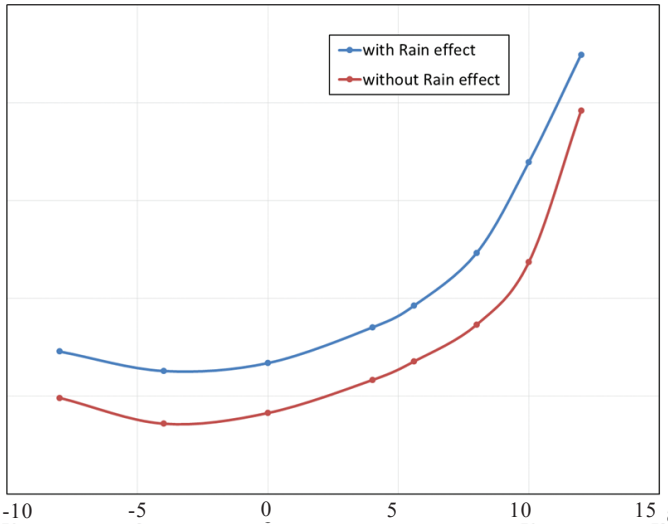

Figure 16. C_D vs. α with & without rain effect for MALE UAV at V = 41.9 m/s, Alt = 3.69 km.

depression convects past the MALE UAV symmetrically, see Fig. 7 & 8. In addition, there is a sudden/abrupt change in rolling and the yawing moment when the localized pressure depression past MALE UAV asymmetrically or on one side of the wing as shown in Fig. 9 & 10. In addition, no change in the yawing and rolling moment is observed when the localized pressure depression convects past the MALE UAV symmetrically.

4.2 Effect of Rain

Simulations in the absence and presence of rain are performed in order to bring out the effect of rain on the aerodynamic characteristics of MALE-UAV. Figure 2 shows the forces and moments convergence in the absence of rain, and Fig. 11 shows their counterparts in the presence of rain.

Figure 12 shows a representative number density contour field of 2 mm droplets dispersed in the flow taken in the symmetry plane. As seen in the figure, the aircraft structure and the alpha at which flies create a shadow zone where the number

Table 3. Delta change in Aerodynamic characteristics for MALE UAV & its % due to rain

α in deg	ΔC_L	ΔC_D	ΔC_m	ΔC_L in %	ΔC_D in %
-8	-0.0467	0.0236	0.0062	40.25	47.95
-4	-0.0426	0.0269	0.0141	-13.72	74.72
0	-0.0153	0.0255	0.0157	-2.05	61.45
4	-0.0054	0.0269	0.0150	-0.47	46.08
5.6	-0.0062	0.0285	0.0104	-0.47	42.00
8	-0.0435	0.0366	-0.0137	-2.90	42.32
10	-0.1208	0.0511	-0.0422	-7.87	43.09
12	-0.1029	0.0286	-0.0404	-7.18	14.62

Table 4. Delta change in inviscid, viscous, and EDP components of lift and drag and its % due to rain.

α in deg	$\Delta C_{L\,inv}$ in %	$\Delta C_{L\,vis}$ in %	$\Delta C_{L\,EDP}$ in %	$\Delta C_{D\,inv}$ in %	$\Delta C_{D\,vis}$ in %	$\Delta C_{D\,EDP}$ in %
-8	-0.0457	0.0025	-0.0035	-0.0014	0.0230	0.0020
-4	-0.0422	0.0016	-0.0020	0.0063	0.0187	0.0019
0	-0.0165	0.0009	0.0003	0.0072	0.0164	0.0019
4	-0.0086	-0.0001	0.0032	0.0079	0.0169	0.0022
8	-0.0105	-0.0006	0.0050	0.0081	0.0180	0.0024
10	-0.0492	-0.0015	0.0072	0.0135	0.0204	0.0028
11	-0.1278	-0.0025	0.0095	0.0253	0.0226	0.0032
12	-0.1093	-0.0033	0.0096	0.0010	0.0243	0.0034

α in deg	$\Delta C_{L\,inv}$ in %	$\Delta C_{L\,vis}$ in %	$\Delta C_{L\,EDP}$ in %	$\Delta C_{D\,inv}$ in %	$\Delta C_{D\,vis}$ in %	$\Delta C_{D\,EDP}$ in %
-8	39.41	-2.13	2.97	-2.81	46.70	4.06
-4	-13.59	0.52	-0.65	17.48	52.05	5.19
0	-2.21	0.12	0.04	17.28	39.63	4.55
4	-0.74	-0.01	0.28	13.47	28.92	3.70
8	-0.80	-0.05	0.38	11.91	26.61	3.49
10	-3.28	-0.10	0.48	15.59	23.54	3.18
11	-8.32	-0.16	0.62	21.31	19.07	2.72
12	-7.62	-0.23	0.67	0.52	12.39	1.72

density of the droplets decreases to a great extent. The sectional C_p plot comparison at α= 8° & 10°, with and without rain effect at the mid-span of the wing, sectional and surface(top) streamlines pattern for the wing are shown in Fig. 13 & 14 respectively. The C_p plot streamlines pattern comparison shows that flow acceleration on the top surface of the wing is less in the presence of rain. Also, the flow separation point on the top surface of the wing along the span is at the forward location. It is due to the accumulation of rain drops on the surface of the wings that will form a wavy and uneven water film, which can effectively roughen the wings and increase skin friction. It can also induce a change in the pressure distribution as seen in Fig. 13 & 14. The aerodynamic characteristics plots (C_L, C_D *vs* α) comparison between MALE UAVs with and without rain effect are shown in Fig. 15 & 16.

Rain can change the external shape of aircraft and in turn, change the aerodynamic characteristics of aircraft[1]. Based

on the CFD analysis carried out, a rainfall rate of 1195 mm/hr is observed to increase the drag and reduce the lift. The rainfall simulated falls under the category of heavy rainfall[1]. It is observed that the drag value is increased by 40 - 60 % in the operating alpha and the alpha stall reduces by 2° because of rain as shown in Figs. 15-16. Table 3 summarises the delta change in force and moment coefficients and its percentage in the presence of rain. Table 4 shows the inviscid, viscous, and EDP component of ΔC_L & ΔC_D and their percentage due to rain respectively. ΔC_L & ΔC_D component in percentage shows the inviscid component of lift reduction is higher than viscous and also a viscous component of drag increase is higher than inviscid.

5. CONCLUSION

The CFD analysis has been carried out to study the effects of propagation of low-pressure depression and rain on the overall aerodynamic characteristics of ADE MALE UAV using CFD++ software. The salient outcomes of this study are summarized in this Technical memo.

- From the low-pressure zone study, it can be observed that the instantaneous rolling moment incremental coefficient can be as high as +/- 0.033 depending on the intensity and relative location of the low-pressure zone w.r.t aircraft. It was observed from flight data analysis, the delta rolling moment due to external disturbance is about -0.05[5]. Due to confidentiality, flight data comparison with CFD data is not presented in detail. This high value of rolling moment may be due to various factors like possible differences in location and intensity of low-pressure air pockets. But based on the simulation study we can conclude that that low-pressure air pocket could have introduced asymmetric rolling moment.
- From the rain simulation study, it is observed that the rain can increase the drag by 40 - 60 % in linear flight operating α, and reduce the stall angle by 2°. Raindrops accumulated on the surface of the wings will form a wavy and uneven water film, which can effectively roughen the wings as well as increase skin friction as well as viscous drag. Also, the roughened wing surfaces certainly induce a change in the pressure distribution due to that there is decrease in the inviscid component of the lift.

  From the study, it was suggested to the pilot (EP/IP) that, to fly UAV in adverse weather effects, a Standard Operating Procedure (SOP) can be adopted such that the aircraft operates with a velocity higher than 1.3 V_{stall} and at power setting not less than 75 % of max power capacity. Delta ROC reduction of 0.6 m/s and delta Endurance reduction of approximately 2.5 – 3.0 hrs was observed at a forward speed of 40-45 m/s, at 20000 feet altitude due to rain for MALE UAV.

REFERENCES

1. Cao, Yihua; Wu, Zhenlong. & Xu, Zhengyu. Effect of rainfall on aircraft aerodynamics. *Progress in Aerospace Sci.,* 2014, **71**, 85-127. doi: 10.1016/j.paerosci.2014.07.003
2. Marshall, J.S. & Palmer, W.M.K. The distribution of raindrops with size. *J. Meteorology,* 1948, **5**(4), 165-166.
3. Joss, J. & Waldvogel, A. Raindrop size distribution and sampling size errors. *J. Atmospheric Sci.,* 1969, **26**(3), 566-569. doi: 10.1175/1520-0469
4. Markowitz, Allan H. Raindrop size distribution Expressions. *J. Appl. Meteorology.,* 1976, **15**(9), 1029-1031.
5. ICFD++ theory manual, Metacomp Technology Inc., www.metacomptech.com (Accessed on 05 October 2022).
6. Girish, Tilokani. & Vijayakumar, M. Post-flight analysis of R-II Ver-3.2, the 19th flight of AF-6, 2019, ADE/AERO/TM/19.
7. Rakesh, G. & Manickam, R. Estimation of aerodynamic moments and winds from flight data of AF-6 DVF19 for the reconstruction of initial roll oscillations in UAV-RTS, 2019, ADE/FSIM/UAV-RTS/TM-2019/03.
8. Vijayakumar, M. Effect of localized pressure depression and rain on Aerodynamic characteristics of R-II MALE UAV, 2019, Technical Memo No.ADE/AERO/TM/19/63.
9. Mahendhran, M. & Balaji, C. Improved efficient modelling of gust flow over flying configurations using overset mesh approach, 21st Annual CFD Symposium, August 8-9, 2019, Bangalore.
10. Wu, Zhenlong; Cao, Yihua. & Ismail, M. Numerical simulation of airfoil aerodynamic penalties and mechanisms in heavy rain. *Int. J. Aerospace Eng.,* 2013. doi: 10.1155/2013/590924
11. Ismail, M.; Cao, Yihua.; Wu, Zhenlong. & Sohail, M.A. Numerical study of aerodynamic efficiency of a wing in simulated rain environment. *J. Aircraft,* 2014, **51**(6).
12. Wu, Z.; Cao, Y. & Yang, Y. Direct CFD prediction of dynamic derivatives for a complete transport aircraft in the dry and heavy rain environment. *The Aeronautical J.,* 2018, **122**(1247), 1-20. doi: 10.1017/aer.2017.121
13. Wu, Zhenlong; Lv, Benin. & Cao, Yihua. Heavy rain effects on aircraft lateral/directional stability and control determined from numerical simulation data. *Aerospace Sci. Technol.* 2018. doi:10.1016/J.AST.2018.07.037
14. Fatahian, Hossein.; Salarian, Hesamoddin.; Nimvari, Majid Eshagh. & Khaleghinia, Jahanfar. Numerical simulation of the effect of rain on aerodynamic performance and aeroacoustic mechanism of an airfoil via a two-phase flow approach. *Springer Nature J.,* 2020. doi: 10.1007/s42452-020-2685-4
15. Sheidani, Armin.; Salavatidezfouli, Sajad. & Schito, Paolo. Study on the effect of raindrops on the dynamic stall of a NACA-0012 airfoil. *J. Brazilian Soc. Mechanic. Sci. Eng.,* 2022, **44**.

CONTRIBUTORS

Mr M. Vijayakumar obtained his M.E. in Aeronautical Engineering from Madras Institute of Technology, Anna University, Chennai and working as Scientist at DRDO-ADE, Bengaluru. His areas of

research include: Adverse weather on aerodynamics characteristics of MALE UAV configuration using CFD approach, 3D RANS code development low reynolds number external flow over single and two-element UAV airfoil & Wing.
In the current study, he has studied the effect of local low-pressure regions in the atmosphere and rain on the aerodynamic characteristics of MALE UAV configuration.

Dr K.M. Parammasivam is a Professor & Head of the Aerospace Engineering Department of MIT, Anna University, Chennai. He obtained PhD from Madras Institute of Technology, Anna University, Chennai, and a Post-doctoral Fellowship from Tokyo Polytechnic University, Japan. His areas of research are computational aerodynamics, combustion, wind energy, and vehicle aerodynamics.
In the current study, he has provided guidance for the adverse weather effect on the Aerodynamics characteristics of UAVs using CFD methodology.

Dr S. Rajagopal is a Scientist and presently the Project Director (of TAPAS UAV) at DRDO-ADE, Bengaluru. He obtained PhD in the area of multidisciplinary optimisation for UAV design from the Indian Institute of Science, Bengaluru.
In the current study, he has provided guidance for the adverse weather on the aerodynamic characteristics of MALE UAVs.

Dr C. Balaji obtained his PhD in Aerospace Engineering from Indian Institute of Technology, Madras. He is currently working as a Senior Scientist at Metacomp Technologies Private Limited Chennai.
In the current study, he provided support on how to use CFD++, a generic flow solver from Metacomp Technologies, to set up the cases covered in the work.